

${}^3\text{He}(p,p){}^3\text{He}$ scattering in the energy range 19 to 48 MeV

B. T. Murdoch,* D. K. Hasell,[†] A. M. Sourkes,[‡] W. T. H. van Oers, and P. J. T. Verheijen
Department of Physics, University of Manitoba, Winnipeg, Manitoba, Canada R3T 2N2

Ronald E. Brown

Los Alamos National Laboratory, Los Alamos, New Mexico 87545

(Received 27 February 1984)

Differential cross sections for ${}^3\text{He}(p,p){}^3\text{He}$ elastic scattering have been measured at 11 energies in the laboratory energy range 19.5 to 47.5 MeV. The most forward c.m. angle for the angular distributions varies from 10.1° to 13.4° , and the most backward angle varies from 163.2° to 173.4° . The relative errors in the data are usually less than 2%, and the scale error is 1.5%. The present data, together with analyzing power and total reaction cross section data of others, have been subjected to an energy-dependent phase shift analysis. The extracted phase shifts and the differential cross sections are compared with the results of a simple resonating-group calculation.

I. INTRODUCTION

The mass-four system is a fundamental one to the study of the nuclear interaction and the internal structure of nuclear systems. The decisive breakthrough in solving the three-body problem, using the integral-equation approach of the Faddeev formulation,¹ has inspired efforts to find adequate extensions for treating more general systems, such as the four-nucleon system. The first results of such rigorous mathematical formulations for interactions involving four nucleons have recently appeared in the literature.²⁻⁶ Data for elastic scattering of protons by ${}^3\text{He}$ in the present energy range should help contribute to these developments.

Furthermore, such data will allow a comparison with, and consequently improvements of, various model dependent descriptions of the static and dynamic properties of four-nucleon systems. For example, for the ${}^4\text{Li}$ nucleus there exist shell-model predictions by Szydlik^{7,8} for the isospin-one, even-parity levels at excitation energies between 45 and 55 MeV (above the ${}^4\text{He}$ ground state). These levels may manifest themselves as resonances in the $p + {}^3\text{He}$ elastic scattering phase shifts. It should be noted that the isospin-one, odd-parity ($l=1$) levels of ${}^4\text{Li}$ have been deduced from $p + {}^3\text{He}$ phase shift analyses at lower energies.

Simple resonating group calculations in the one channel approximation⁹ have resulted in predictions of the $p + {}^3\text{He}$ phase shifts for proton energies between 0.5 and 40 MeV with l values up to 6. It is expected that the inclusion of a phenomenological imaginary potential in such calculations (as, for instance, has been done¹⁰ for the case $p + {}^4\text{He}$) will improve agreement with the experimental differential cross sections in the higher energy region. A detailed comparison between improved resonating-group theoretical predictions and the experimental angular distributions may lead to a better understanding of cluster configurations in these very light nuclear systems. Conversely, the resonating-group phase shifts are useful as starting values in a refined phase shift analysis of the

$p + {}^3\text{He}$ elastic scattering data.

There has been in the last decade a large accumulation of $p + {}^3\text{He}$ elastic scattering data, although mainly in the energy region below 20 MeV. In particular, many observables have been measured at an incident proton energy of 19.5 MeV. The highest precision differential cross section data are those of Hutson *et al.*¹¹ covering the range of c.m. angles between 16° and 172° with absolute uncertainties of about 1%. Morales *et al.*^{12,13} measured differential cross sections for 12 energies from 18 to 57 MeV with typical absolute uncertainties of 4% to 9%. At 30.6 and 49.5 MeV, Harbison *et al.*¹⁴ measured differential cross sections as well as polarizations over a wide angular range with uncertainties from 5% to 15%.

Several groups have made phase-shift analyses of $p + {}^3\text{He}$ elastic scattering in this energy range. For example, at 19.5 MeV, Baker *et al.*¹⁵ measured the proton and ${}^3\text{He}$ analyzing powers as well as the spin-spin correlation parameters A_{yy} and A_{xx} in $p + {}^3\text{He}$ elastic scattering. These authors made a phase-shift analysis of their data and the 19.5 MeV differential-cross-section data of Morales *et al.*¹³ They included partial waves up to $l=4$ and two coupling parameters, but ignored absorption effects. It was apparent from inspection of their results that better quality cross-section data would be very important for an extension of the phase-shift analysis to higher energies. Morales *et al.*¹³ made phase-shift analyses of the available data at several energies in the range from 18 to 35 MeV. While the resulting phase shifts for $l=0, 1,$ and 2 show a reasonable behavior as a function of energy, there still exists considerable scatter of the individual phase-shift values attributable in part to data of insufficient accuracy and quantity. Harbison *et al.*¹⁴ have fitted their differential cross section and polarization angular distributions at 30.6 and 49.5 MeV quite satisfactorily. However, the substantial uncertainties in their data, the limited input to the phase-shift analysis, and the single-energy approach make their phase-shift solutions somewhat ambiguous. A similar remark about the phase-shift solution can be made with regard to the analyses of

Darves-Blanc *et al.*¹⁶ at 30 MeV, and of Müller *et al.*¹⁷ at 25 and 30 MeV.

In the energy region below 20 MeV, Hale *et al.*¹⁸ performed an energy-dependent phase-shift analysis using an *R*-matrix parametrization. One of the purposes of the study of the $p + {}^3\text{He}$ system undertaken at the University of Manitoba Cyclotron Laboratory is to extend these types of analyses into the higher-energy region. Thus, measurements were first made¹⁹ of the $p + {}^3\text{He}$ total reaction cross section σ_R at ten energies in the range 18 to 48 MeV. The second phase of this work is reported in this paper, which describes accurate measurements of elastic differential cross sections at 11 energies from 19.5 to 47.5 MeV over the approximate angular range 10° to 173° (c.m.). While this work was in progress, Watson *et al.*²⁰ measured the proton analyzing powers A_y at 21.4, 24.8, 27.3, and 30.1 MeV and Birchall *et al.*²¹ measured the proton analyzing powers A_y at 32.5, 35.0, 37.5, 40.0, 45.0, and 49.6 MeV using the polarized proton beam at the Berkeley 88-inch cyclotron. It was felt worthwhile to attempt a fit to the first three data sets just mentioned using the Los Alamos *R*-matrix code EDA,²² and such a fit is reported here. Also, the present differential cross sections and some of the extracted phase shifts are compared with the results of a simple resonating-group calculation.

Further experiments are in progress at Manitoba, using a polarized ${}^3\text{He}$ target, to obtain more information on spin-dependent observables. Such information is very much needed to perform a more definitive phase-shift analysis in this energy range.

II. EXPERIMENT

The experiment was performed using the momentum-analyzed proton beam of the University of Manitoba sector-focused cyclotron. The momentum analysis was accomplished by means of a 45° bend through an analyzing magnet, which was calibrated by using the kinematic crossover method²³ and by observing the well-known $J^\pi = \frac{3}{2}^+$ second excited state in ${}^7\text{Li}$ at 16.68 MeV in $p + {}^4\text{He}$ scattering.²⁴ The incident beam energy was known to within 100 keV and had a spread of about 150 keV (FWHM).

The scattering chamber used has an inner diameter of 115 cm and contains a movable array of eight detectors at 10.00° intervals, thus spanning a range of 70° . The angle extremes capable of being reached are 7.5° in the forward hemisphere and 170° in the backward hemisphere, and the array can be positioned to an accuracy of 0.01° . The detector positions with respect to one another are known to 0.02° . Thus, a contribution to the relative error of 0.03° times the slope of the cross section was included. The detectors used were either silicon surface barrier or NaI(Tl) scintillation detectors, depending on the energy of the scattered protons.

The ${}^3\text{He}$ target gas of better than 99.8% purity (less than 0.1% ${}^4\text{He}$ and less than 0.1% H_2 and N_2 impurities) was contained in a cylindrical cell 8.6 cm in diameter with a window 1.6 cm high extending over a 275° angular range and covered by 50- μm thick kapton foil. The ${}^3\text{He}$ gas in the cell was kept at a pressure of about 1.5 atm and

flushed regularly to prevent the buildup of contaminants. A thermistor, calibrated to 0.1%, was embedded in the lid of the cell and allowed the temperature to be read to a relative accuracy of ± 0.5 K. A Wallace-Tiernan gauge, model FA141, calibrated to 0.5%, was used to read the pressure to a relative accuracy of ± 2.5 Torr.

The gas scattering geometry was defined by means of parallel-sided front slits at a distance of 5.471 ± 0.005 cm from the scattering chamber center and rectangular rear apertures at a distance of 32.768 ± 0.008 cm. Antiscattering baffles were mounted between the front and rear geometry-defining apertures. The rear apertures were fabricated using spark erosion techniques and their areas (typically 0.46 cm wide by 1.25 cm high) are known to better than 0.25%.

A calibrated Brookhaven Instruments Current Integrator (model 1000) was used for charge integration, with electron suppression on the carbon-lined 1.74 m long Faraday cup ensuring accurate particle collection. Because of the possible presence of a small beam halo to the incident proton beam, the uncertainty in the beam integration was conservatively taken to be $\pm 0.5\%$ relative and $\pm 1.2\%$ absolute. The direction of the incident beam was periodically monitored by means of detectors having nearly identical geometry and viewing particles scattered from a Ni foil at 15.0° left and right of the incident beam. The beam cross section at the center of the scattering chamber was typically 0.3 cm wide by 0.8 cm high.

Cross sections were measured successively left and right of the incident beam direction and then averaged in order to cancel out any first order effects which would have resulted from the beam being either off-center at the target or not quite coincidental with the chamber axis. This averaging procedure can also be shown to cancel practically all error which could result from a systematic deviation in the scattering angles. Pulse-height spectra were accumulated by standard electronic techniques using analog-to-digital converters (ADC's) and a PDP-15 computer system and were recorded on magnetic tape. For further details regarding the experimental arrangement and procedure, see Ref. 25.

III. DATA REDUCTION

The data recorded on magnetic tape were reduced to differential cross sections in two steps. First, uncorrected differential cross sections were obtained, and second, the necessary corrections were applied. The proton elastic scattering peaks were resolved from the spectra by subtracting the background using smooth background functions, and at extreme forward angles, by subtracting the contributions from the small amount of impurities present in the gas cell. The statistical error in the yield includes the error in the background subtraction. The uncertainty both in the subtraction of contaminant yields and in the dead-time correction was taken to be 20% of the correction.

Three further corrections were applied to the data for (i) the effects of multiple scattering in the gas and exit foil of the target cell, (ii) the loss of elastically scattered protons in the detector material due to nuclear reactions, and

TABLE I. Contributions to the relative uncertainties in the differential cross sections.

Type of uncertainty	Uncertainty
Counting statistics (including background subtraction)	<1% (except at 40 MeV)
Dead time correction	$\pm 20\%$ of the correction
Subtraction of contaminant yields	$\pm 20\%$ of the correction
Integration of beam current	$\pm 0.5\%$
Detector angle	$\pm 0.03^\circ$
Pressure	± 2.5 Torr
Temperature	± 0.5 K
Finite geometry correction	$\pm 0.1\%$

(iii) the effects of finite geometry. The corrections for multiple scattering were estimated using the expression given by Chase and Cox²⁶ and were found to be very small. The fraction of protons lost from the elastic peak in the spectra because of nuclear reactions in the detectors was interpolated from the published results²⁷ for NaI and Si. The fraction for NaI varied between 0.5% at 21 MeV and 2.9% at 50 MeV with an absolute uncertainty of $\pm 0.04\%$. The finite geometry corrections take into account that the measurements were done with a finite solid angle, with a beam of finite size traversing a gas target, and with a beam which in first approximation converges towards the target. The finite geometry correction factor of Kan²⁸ was adapted to the particular conditions of the present experiment. The maximum correction occurred at forward angles, but was always less than 1%. The various contributions to the relative error in the cross sections are indicated in Table I, and the contributions to the scale error are given in Table II. Except for the 40-MeV angular distribution, the relative errors are mostly smaller than 2%, and the scale error is 1.5%.

IV. EXPERIMENTAL RESULTS

In Fig. 1 are shown the present measurements at 19.5 MeV along with the results of Ref. 11 at 19.48 MeV. It is seen that the two data sets agree quite well. In Fig. 2 are shown the present measurements at 30.0 MeV along with the results of Ref. 13 at 30.0 MeV and the results of Ref. 14 at 30.6 MeV. The latter two data sets show more scatter than the present set, as is to be expected because of their larger quoted experimental uncertainties.

Our complete set of measurements is shown in Figs. 3 and 4. The differential cross sections at 19.5, 21.3, 25.0,

27.5, and 30.0 MeV are illustrated in Fig. 3, and those at 32.4, 35.0, 37.5, 40.0, 45.0, and 47.5 MeV are plotted in Fig. 4. The errors are usually smaller than the size of the plotting symbols. Note that data were taken at 2.5° intervals at forward angles and 5° intervals at backward angles. The occasional gaps which appear in the angular distributions were caused by a deterioration in some of the NaI(Tl) detectors during data taking. The angular distributions show a smooth behavior as a function of energy, with a characteristic minimum near 120° which results from the interference between forward-peaked direct processes and backward-peaked exchange processes.^{29,30} The consistency of these angular distributions has been demonstrated recently,³¹ as a single-energy phase shift analysis involving all available polarization data resulted in good fits (reduced χ^2 of unity; and for the cross sections alone, a χ^2 per data point of typically 0.8). The Coulomb-nuclear interference region occurs at too small an angle to be studied in any great detail with the present experimental arrangement. Data tables are available in a Los Alamos report.³²

V. PHASE-SHIFT ANALYSIS

As was mentioned in Sec. I, the present differential cross sections $\sigma(\theta)$, the proton analyzing powers A_y of Ref. 20, and the total reaction cross sections σ_R of Ref. 19 (a grand total of 593 data points) were subjected to an energy-dependent phase-shift analysis using the Los Alamos code EDA.^{22,33} This analysis has also been mentioned in Refs. 34 and 35. The code EDA is very general in its handling of the spin structure of nuclear reactions, but does require the user to employ the parametrization of the R -matrix formalism.³⁶ This formalism has the advan-

TABLE II. Contributions to the uncertainty in the absolute scale of the differential cross sections.

Type of uncertainty	Uncertainty
Pressure	$\pm 0.5\%$
Temperature	$\pm 0.1\%$
Geometry factor	$\pm 0.5\%$
Gas purity	$\pm 0.1\%$
Integration of the beam current	$\pm 1.2\%$
Energy of the incident proton beam	$\pm 0.4\%$
Energy-degraded-proton contamination of the incident beam	<0.1%
Correction for reactions in the NaI(Tl) or Si detectors	$\pm 0.04\%$

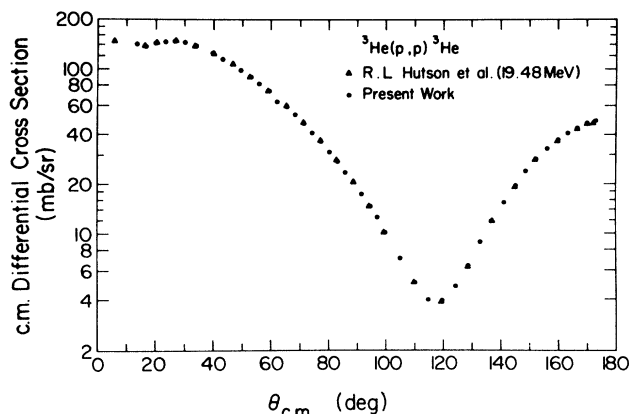


FIG. 1. Present $p + {}^3\text{He}$ elastic differential cross section at a laboratory proton energy of 19.5 MeV and the measurements of Ref. 11 at 19.48 MeV.

tage of imposing unitarity on the analysis and is especially useful when the data display readily identifiable resonant structure. With care it can also be used in cases of less obvious structure, where the analysis is initialized with the poles of the R matrix outside of the energy region of interest.

Partial waves through $l=7$ were allowed in the elastic channel; however, it should be stressed that the penetrabilities which occur in a natural way in the R -matrix method allow the higher partial waves to be effective only at the higher energies. Because the R -matrix formalism is unitary, the effect of reactions (absorption) on the elastic scattering can only be accounted for through the inclusion of specific reaction channels in the analysis, in contrast to the use of complex phase shifts in the more usual type of analysis. Absorption was therefore incorporated (through $l=6$ only) by including $d + pp$ and $d^* + pp$ as two-body channels, the latter being coupled only to the 1S_0 elastic channel. Of course, only the total strength to these channels is constrained in the parameter search by the total reaction cross section, σ_R , as is also the case in the complex-phase method. Spin (s) and total-angular-momentum (j) splittings were allowed through $l=5$. In

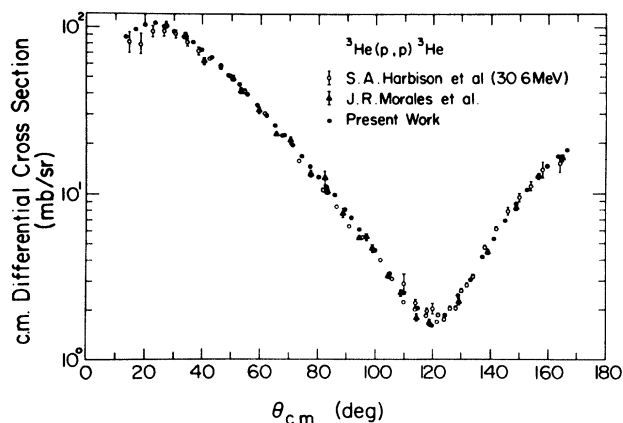


FIG. 2. Present $p + {}^3\text{He}$ elastic differential cross section at a laboratory proton energy of 30.0 MeV, the measurements of Ref. 13 at 30.0 MeV, and the measurements of Ref. 14 at 30.6 MeV.

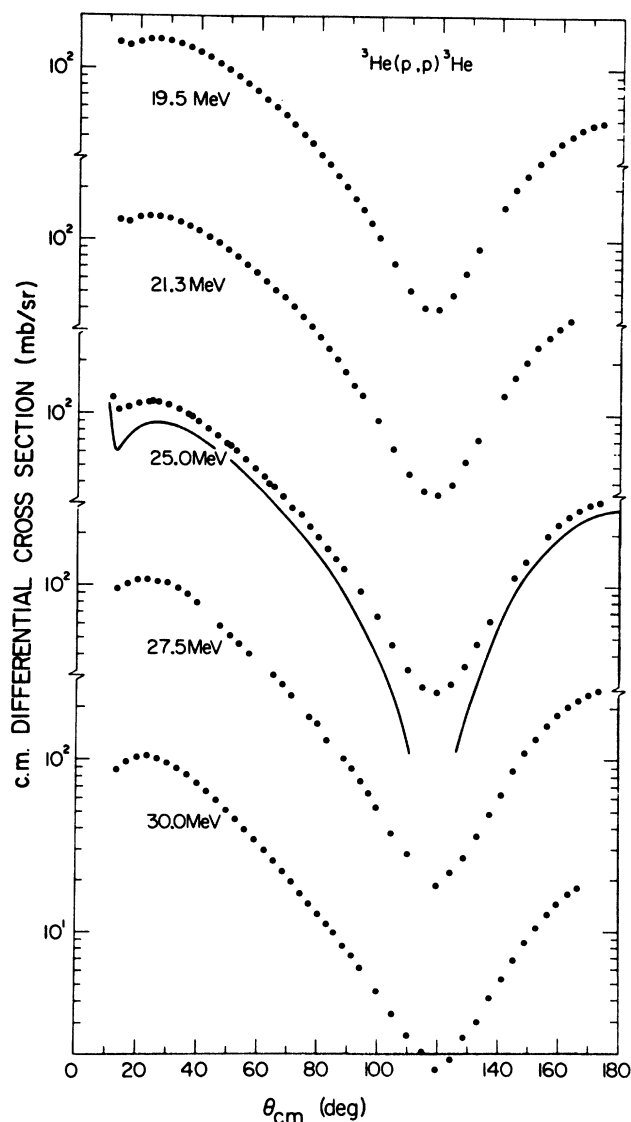


FIG. 3. Present $p + {}^3\text{He}$ elastic differential cross sections (points) at the indicated laboratory proton energies. The curve at 25.0 MeV shows the result of a simple resonating-group calculation.

the initial part of the parameter search there were no couplings among the elastic states, but as the search progressed singlet-triplet spin couplings were introduced for $l=1$ and 2, and orbital-angular momentum couplings $l \rightarrow l+2$ were introduced for $l=0, 1$, and 2. The elastic states and their mutual couplings are depicted in Fig. 5.

To try to avoid imposing, *ab initio*, structure on the phase-shift solutions due to the nature of the R -matrix approach, the initial parametrization was chosen to yield a smooth, structureless dependence on energy for the phase shifts (similar to 3S_1 in Fig. 6) and phase-shift values at 20 MeV close to those from the low-energy analysis of Ref. 18. This usually was accomplished by including from 1 to 3 broad levels in the R matrix associated with a reaction submatrix of a given total angular momentum and parity; however, as many as four levels were used for some of the submatrices containing low par-

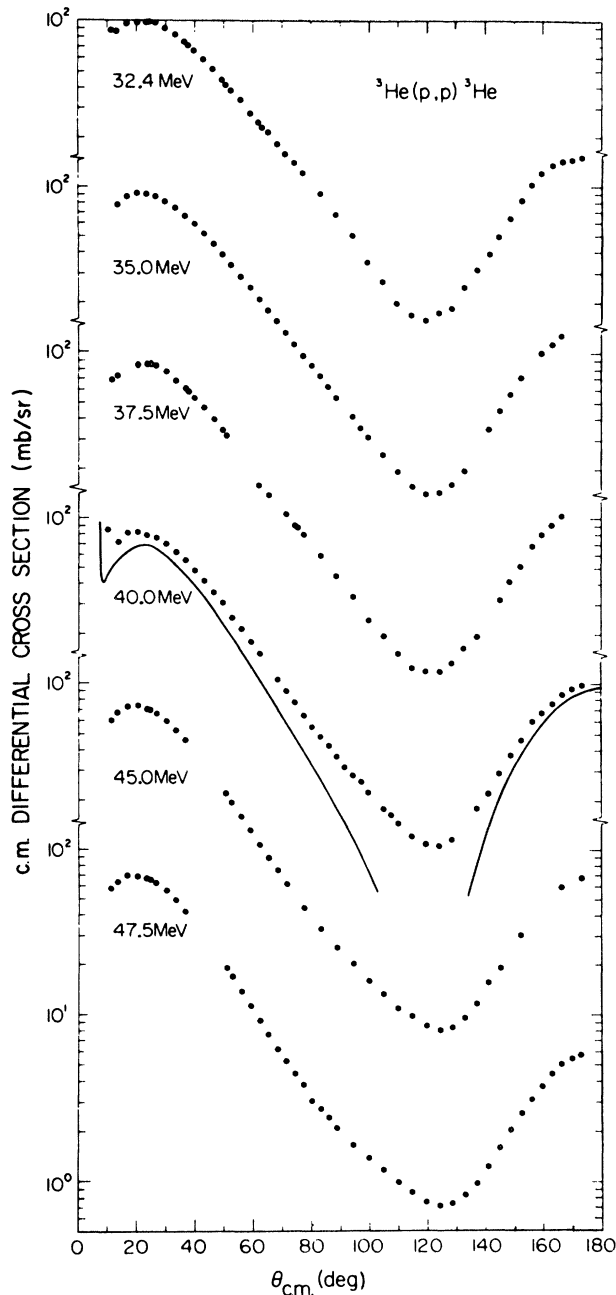


FIG. 4. Present $p + {}^3\text{He}$ elastic differential cross sections (points) at the indicated laboratory proton energies. The curve at 40.0 MeV shows the result of a simple resonating-group calculation.

tial waves. At the beginning of the parameter search about 60 parameters were varied, with this being increased to about 120 during the middle phases of the search and being decreased to about 80 toward the end. A χ^2 minimum was found with a χ^2 per datum of 1.08. Although no attempt was made to constrain the 20 MeV phases during the search, their final values showed an average absolute deviation of only 7° from those of Ref. 18. This bodes well for a planned²² analysis covering the entire range 0 to 50 MeV. The curves in Fig. 6 show the phase shifts from our analysis for the first four partial

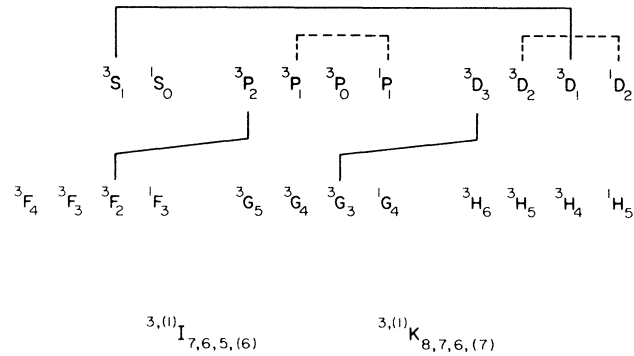


FIG. 5. Elastic states $2s+1L_J$ used in the phase-shift analysis. The elastic couplings used in the present phase-shift analysis are shown by solid and dashed lines.

waves. The phase shifts are simply related to the elements S of the S matrix by $S = |S| \exp(2i\delta)$, where the amplitude $|S|$ and phase δ are real numbers. Note that we have not made any Blatt-Biedenharn³⁷ type of transformation of S , and hence there are no “eigenphases” or “mixing parameters” in our description. The values of $|S|$ are determined in our analysis by σ_R ,¹⁹ which varies smoothly from 40 mb near 19 MeV to 125 mb near 48 MeV. These relatively small values, along with their monotonic energy dependence, yield rather smooth energy behavior for $|S|$ (see Fig. 7). For only three states does $|S|$ become smaller than 0.8; these are 1D_2 (0.74), 3P_2 (0.63), and 3S_1 (0.58), where the minimum values attained by $|S|$ over the energy range 19 to 48 MeV have been indicated in parentheses.

In a multichannel, multilevel R -matrix analysis it is nearly impossible to relate directly the parameters of the R matrix to the physics of the reaction, except perhaps for levels that generate very narrow resonance structures. The key to the physics is in the S matrix, which is derivable from the R matrix in a complicated way.³⁸ It is therefore difficult to extract from the analysis the structure of S expressed, say, in terms of its poles and residues, and one must be satisfied with presenting S graphically in Figs. 6 and 7.

Quantitative results of this analysis should be approached with caution because of possible pitfalls and inherent limitations in applying the R -matrix approach, and the lack of sufficient spin dependent data. However, some features of Fig. 6 are worth noting. The broad structure in the singlet phases is striking. The singlet S phase deviates from the smooth behavior exhibited by the triplet S phase. Also, excursions in the D waves are significantly larger than those in the F waves and are comparable to those in the P waves. Structure in the positive-parity partial waves could possibly be explained by shell model calculations^{7,8} that predict positive-parity levels in this energy range.

Attempts were made to fit the data in the 30 to 50 MeV range with a standard optical model, which does not treat the full spin structure of the p - ${}^3\text{He}$ system. Poor results were obtained, with values of χ^2 per datum in the hundreds. It was therefore deemed meaningless to try to

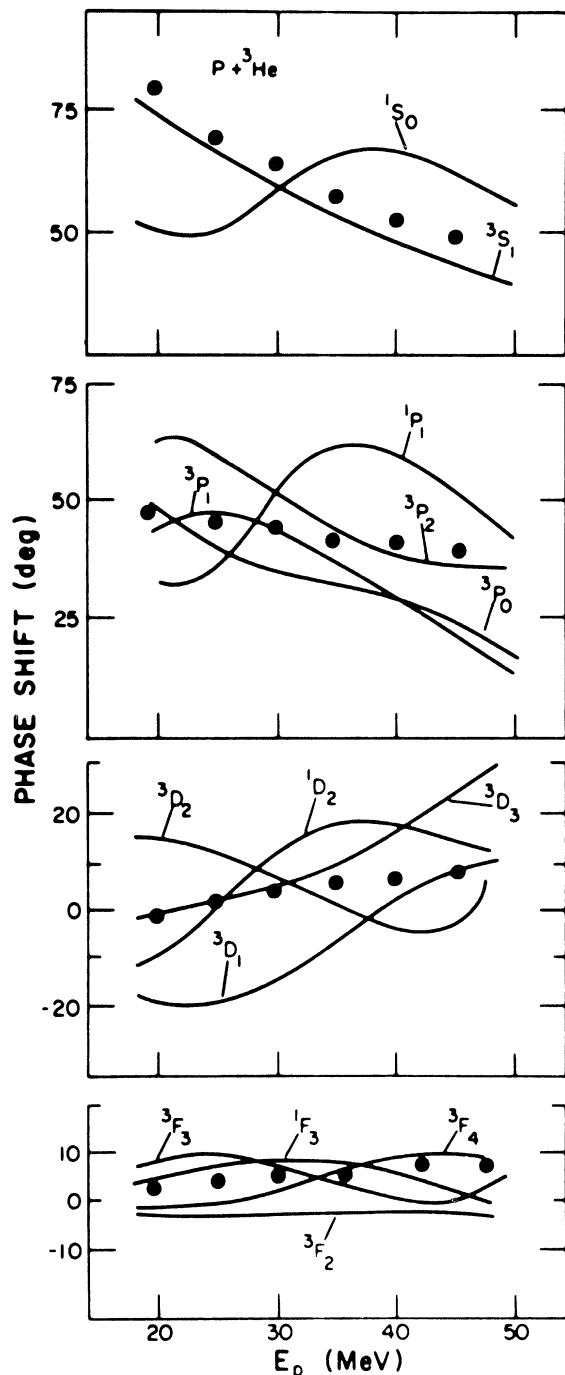


FIG. 6. Phase shifts (curves) through $l=3$ vs proton laboratory energy E_p from the present analysis. The points are the triplet phases from a simple resonating-group calculation.

compare those results with the present phase-shift analysis.

VI. RESONATING-GROUP CALCULATIONS

A simple resonating-group³⁹ calculation was performed to compare with the present results. The computer code for the single-channel $p + {}^3\text{He}$ calculation of Ref. 9 was modified⁴⁰ to include the Coulomb-exchange terms and a

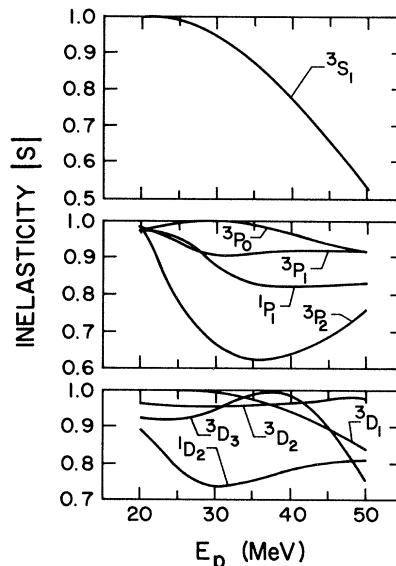


FIG. 7. Inelasticity parameters (curves) through $l=2$ vs proton laboratory energy E_p from the present analysis. The 1S_0 inelasticity (not shown) is essentially unity over the entire energy range displayed.

phenomenological imaginary potential to account approximately for the effects of reactions on the elastic channel. The calculation employs a two-Gaussian wave function for the ${}^3\text{He}$ nucleus which reproduces reasonably well the properties of ${}^3\text{He}$. A purely central nucleon-nucleon force is used which fits the singlet and triplet two-nucleon scattering lengths and effective ranges. This force also includes a space-exchange mixture described by a parameter u such that $u=1$ corresponds to a Serber force. In the present calculation the strength of the imaginary potential was adjusted at each energy to reproduce the measured¹⁹ total reaction cross section, and u was set equal to 1. The resulting triplet phase shifts are shown as dots in Fig. 6; the singlet phases are not a great deal different from, and show a similar trend to, the triplet phases. The agreement of the calculated triplet phases with the empirical ones seems reasonably good, considering the fact that only a central nucleon-nucleon force was used. It is clear that to learn anything further from the calculation it must be improved to include noncentral parts of the nucleon-nucleon force, as, for example, has been done by Heiss and Hackenbroich⁴¹ for the $p + {}^3\text{He}$ system at lower energies.

Examples of the calculated differential cross sections are shown in Figs. 3 and 4 at 25.0 and 40.0 MeV, respectively. The results at other energies are similar; that is, the calculated cross sections are too low, and the calculated interference minimum is much too deep. The latter problem is caused by the neglect of noncentral forces and has been commented on, for example, in Ref. 42. The former problem could be alleviated somewhat by making some minor adjustments in the present calculation. For example, if the exchange mixture in the nucleon-nucleon force were changed from pure Serber by increasing the parameter u , then the calculated cross section would become larger. However, there is little point to such manipulations with the calculation in its present simple form.

VII. CONCLUSION

Here are reported measurements of $p + {}^3\text{He}$ elastic differential cross sections $\sigma(\theta)$ over the proton bombarding energy range 19 to 48 MeV. These data, combined with total reaction cross sections¹⁹ σ_R and proton analyzing powers²⁰ A_y , measured by others, were subjected to an energy-dependent phase-shift analysis using the Los Alamos R -matrix code.^{22,33} The analysis yielded phases in positive parity waves having some interesting energy structure, corroborated by the results of a single-energy phase shift analysis, to be reported on elsewhere.³¹ There is reasonable agreement between the present results and those of a simple resonating-group calculation; however,

more theoretical effort is needed in order to understand the $p + {}^3\text{He}$ data in the present energy range in terms of the basic nucleon-nucleon force. We conclude by reemphasizing the need for more spin-dependent data for the $p + {}^3\text{He}$ system, especially above 20 MeV.

ACKNOWLEDGMENTS

The authors thank J. W. Watson for the use of the proton analyzing-power data prior to publication and express gratitude to G. M. Hale and D. C. Dodder for help in using their code EDA. This work was supported in part by the Natural Sciences and Engineering Research Council of Canada and the United States Department of Energy.

*Present address: Schlumberger Well Services, Inc., Houston, TX 77023.

†Present address: Rutherford Appleton Laboratory, Chilton, Didcot OX11 0QX, England.

‡Present address: Manitoba Cancer Treatment and Research Foundation, Winnipeg, Manitoba, Canada R3E 0V9.

¹L. D. Faddeev, *Zh. Eksp. Teor. Fiz.* **39**, 1459 (1960) [*Sov. Phys.—JETP* **12**, 1014 (1961)].

²W. Sandhas, in *Few Body Dynamics*, edited by A. N. Mitra, I. Slaus, V. S. Bhasin, and N. K. Gupta (North-Holland, Amsterdam, 1976), p. 540.

³R. Perne and W. Sandhas, *Phys. Rev. Lett.* **39**, 788 (1977).

⁴H. Kroger and W. Sandhas, *Phys. Rev. Lett.* **40**, 834 (1978).

⁵R. Perne and W. Sandhas, in *Proceedings of the Eighth International Conference on Few Body Systems and Nuclear Forces II*, edited by H. Zingl, M. Haftel, and H. Zankel (Springer, Berlin, 1978), p. 263.

⁶A. C. Fonseca, *Phys. Rev. C* **10**, 1711 (1979).

⁷P. P. Szydluk, *Phys. Rev. C* **1**, 146 (1970).

⁸P. P. Szydluk, J. R. Borowicz, and R. F. Wagner, *Phys. Rev. C* **6**, 1902 (1972).

⁹I. Reichstein, D. R. Thompson, and Y. C. Tang, *Phys. Rev. C* **3**, 2139 (1971).

¹⁰D. R. Thompson, Y. C. Tang, and R. E. Brown, *Phys. Rev. C* **5**, 1939 (1972).

¹¹R. L. Hutson, N. Jarmie, J. L. Detch, Jr., and J. H. Jett, *Phys. Rev. C* **4**, 17 (1971).

¹²J. R. Morales, Ph.D. thesis, University of California, Davis, 1970 (unpublished).

¹³J. R. Morales, T. A. Cahill, D. J. Shadoan, and H. Willmes, *Phys. Rev. C* **11**, 1905 (1975).

¹⁴S. A. Harbison, R. J. Griffiths, N. M. Stewart, A. R. Johnston, and G. T. A. Squier, *Nucl. Phys.* **A150**, 570 (1970).

¹⁵S. D. Baker, T. A. Cahill, P. Catillon, J. M. Durand, and D. Garreta, *Nucl. Phys.* **A160**, 428 (1971).

¹⁶R. Darves-Blanc, Nguyen Van Sen, J. Arvieux, J. C. Gondrand, A. Fiore, and G. Perrin, *Nucl. Phys.* **A191**, 353 (1972).

¹⁷D. Müller, R. Beckmann, and U. Holm, *Nucl. Phys.* **A311**, 1 (1978).

¹⁸G. M. Hale, J. J. Devaney, D. C. Dodder, and K. Witte, *Bull. Am. Phys. Soc.* **19**, 606 (1974); G. M. Hale (private communication).

¹⁹A. M. Sourkes, A. Houdayer, W. T. H. van Oers, R. F. Carlson, and R. E. Brown, *Phys. Rev. C* **13**, 451 (1976).

²⁰J. W. Watson, H. E. Conzett, R. M. Larimer, B. T. Leemann, and E. J. Stephenson, *Bull. Am. Phys. Soc.* **22**, 531 (1977); J.

W. Watson (private communication).

²¹J. Birchall, W. T. H. van Oers, H. E. Conzett, P. von Rossen, R. M. Larimer, J. W. Watson, and R. E. Brown, in *Polarization Phenomena in Nuclear Physics—1980* (Fifth International Symposium, Sante Fé), Proceedings of the Fifth International Symposium on Polarization Phenomena in Nuclear Physics, AIP Conf. Proc. No. 69, edited by G. G. Ohlsen, R. E. Brown, N. Jarmie, M. W. McNaughton, and G. M. Hale (AIP, New York, 1981), p. 1263.

²²G. M. Hale and D. C. Dodder (private communication).

²³B. M. Bardin and M. E. Rickey, *Rev. Sci. Instrum.* **35**, 902 (1964); R. Smythe, *ibid.* **35**, 1197 (1964).

²⁴P. Darriulat, D. Garreta, A. Tarrats, and J. Testoni, *Nucl. Phys.* **A108**, 316 (1968); S. N. Bunker, J. M. Cameron, M. B. Epstein, G. Paic, J. R. Richardson, J. G. Rogers, P. Tomaš, and J. W. Verba, *ibid.* **A133**, 537 (1969).

²⁵A. Houdayer, N. E. Davison, S. A. Elbaker, A. M. Sourkes, W. T. H. van Oers, and A. D. Bacher, *Phys. Rev. C* **16**, 1985 (1978).

²⁶C. T. Chase and R. T. Cox, *Phys. Rev.* **58**, 243 (1940).

²⁷A. M. Sourkes, M. S. de Jong, C. A. Goulding, W. T. H. van Oers, E. A. Ginkel, R. F. Carlson, A. J. Cox, and D. J. Margaziotis, *Nucl. Instrum. Methods* **143**, 589 (1977); M. O. Makino, C. N. Waddell, and R. M. Eisberg, *ibid.* **60**, 109 (1968).

²⁸J. T. C. Kan, *Rev. Sci. Instrum.* **44**, 323 (1973).

²⁹M. LeMere, R. E. Brown, Y. C. Tang, and D. R. Thompson, *Phys. Rev. C* **12**, 1140 (1975).

³⁰D. R. Thompson, R. E. Brown, M. LeMere, and Y. C. Tang, *Phys. Rev. C* **16**, 1 (1977).

³¹P. J. T. Verheijen, Ph.D. thesis, University of Manitoba, Winnipeg, 1983 (unpublished); P. J. T. Verheijen, R. H. McCamis, and W. T. H. van Oers (unpublished).

³²R. E. Brown, B. T. Murdoch, D. K. Hasell, A. M. Sourkes, and W. T. H. van Oers, Los Alamos Scientific Laboratory Report No. LA-8179-MS, 1980 (unpublished). Note that the tables in this report have since been revised. This refers to nine data points in total at laboratory angles $\geq 80^\circ$ and energies of 32.4 and 37.5 MeV.

³³The use of this code to study the $p + {}^4\text{He}$ system is described in D. C. Dodder, G. M. Hale, N. Jarmie, J. H. Jett, P. W. Keaton, Jr., R. A. Nisley, and K. Witte, *Phys. Rev. C* **15**, 518 (1977).

³⁴R. E. Brown, in *Clustering Aspects of Nuclear Structure and Nuclear Reactions* (Winnipeg, 1978), Proceedings of the Third International Conference on Clustering Aspects of Nuclear Structure and Nuclear Reactions, AIP Conf. Proc. No. 47,

- edited by W. T. H. van Oers, J. P. Svenne, J. S. C. McKee, and W. R. Falk (AIP, New York, 1978), p. 90.
- ³⁵R. E. Brown, B. T. Murdoch, D. K. Hasell, A. M. Sourkes, and W. T. H. van Oers, see Ref. 5, p. 292.
- ³⁶A. M. Lane and R. G. Thomas, *Rev. Mod. Phys.* 30, 257 (1958).
- ³⁷J. M. Blatt and L. C. Biedenharn, *Rev. Mod. Phys.* 24, 258 (1952).
- ³⁸G. M. Hale, in *Neutron Standards and Applications* (National Bureau of Standards, Gaithersburg, MD, 1977), p. 30.
- ³⁹Y. C. Tang, M. LeMere, and D. R. Thompson, *Phys. Rep.* 47, 167 (1978).
- ⁴⁰M. LeMere (private communication).
- ⁴¹P. Heiss and H. H. Hackenbroich, *Nucl. Phys.* A182, 522 (1972).
- ⁴²I. Reichstein and Y. C. Tang, *Nucl. Phys.* A158, 529 (1970).